

Experiments at High-Energy e^+e^- -Colliders

D. Schulte

Abstract

Linear e^+e^- colliders are the most promising candidates for the next generation of lepton colliders. They will allow physics investigations complementary to the LHC, with a centre-of-mass energy ranging from the Z^0 mass to 5 TeV, depending on the project. A short overview over the main studies—TESLA, JLC, NLC and CLIC—is given, emphasising the reasoning that has driven their choices. The strong beam-beam interaction leading to a pinch effect and to beamstrahlung is briefly mentioned, together with its effect on luminosity and luminosity spectrum. The possible tradeoff between the latter two is illustrated. At high centre-of-mass energies, also coherent pair creation influences the beam-beam interaction and requires careful detector design to avoid severe background. Also at low energies incoherent pair creation is a significant background source, its effects on the designs of the vertex detector and the masking system are described. Very briefly additional background sources due to two photon production of hadrons and due to neutrons are mentioned.

1 Introduction

The LHC will allow the investigation of particle physics on the multi-TeV scale. However, the next generation of high-energy electron-positron linear colliders with a centre-of-mass energy E_{cm} in the range of up to one TeV can provide a number of interesting complementary experiments [1], mainly precision measurements.

Several possible linear colliders are being studied at the moment, covering centre-of-mass energies from the Z^0 -mass to 5 TeV. TESLA [2] is a superconducting machine aimed to give very high luminosity at centre-of-mass energies up to 0.8 TeV. NLC [3] is a normal conducting machine with an acceleration frequency in the X-band, which is mainly investigated at SLAC. JLC-X [4] is a very similar design studied at KEK. Some effort is being taken to combine the last two studies, for example a common parameter set for the beams at the interaction point exists. These machines are designed for $E_{cm} = 1$ TeV and should be extendable to $E_{cm} = 1.5$ TeV. JLC-C is a backup study at half the X-band frequency, also studied at KEK with $E_{cm} = 0.5$ TeV. CLIC [5], a very high frequency machine, is investigated at CERN. It is aimed at $E_{cm} = 3$ TeV with a possible upgrade to $E_{cm} = 5$ TeV. An effort to compare the designs on a technical basis and to keep up to date information on all projects is made by the International Linear Collider Technical Review Committee [6].

Two joint studies by ECFA and DESY on the physics and detectors at TESLA have taken place [7] [2] [8]. Other studies have been performed for the NLC [9] and JLC [10]. All of these will join the Worldwide Study of the Physics and Detectors for Future Linear e^+e^- Colliders [11].

In the following, an introduction into the conditions for experiments at linear colliders is given rather than into the experiments themselves. First the constraints

Table 1: The parameters for the main projects at different centre-of-mass energies. For NLC/JLC also sets for $E_{cm} = 1.5$ TeV exist.

name		TESLA		NLC/JLC		CLIC			
E_{cm}	[TeV]	0.5	0.8	0.5	1.0	0.5	1.0	3.0	5.0
\mathcal{L}	$[10^{34} \text{cm}^{-2} \text{s}^{-1}]$	3.1	5.0	0.65	1.3	0.63	1.36	14.6	24.6
f_{RF}	[GHz]	1.3	1.3	11.4	11.4	30	30	30	30
G_{load}	[MV/m]	21.7	34	55	55	100	100	150	200
η	[%]	23	18	8.9	8.6	14.2	14.2	10.7	7.8
f_r	[Hz]	5	3	120	120	200	100	75	50
N_b		2820	4500	95	95	150	150	150	150
Δ_b	[ns]	337	189	2.8	2.8	0.67	0.67	0.67	0.67
N	$[10^{10}]$	2.0	1.4	0.95	0.95	0.4	0.4	0.4	0.4
σ_z	$[\mu\text{m}]$	400	300	120	120	50	50	30	25
ϵ_x	$[\mu\text{m}]$	10	8	4.5	4.5	1.88	1.48	0.6	0.58
ϵ_y	$[\mu\text{m}]$	0.03	0.01	0.1	0.1	0.1	0.07	0.01	0.01
σ_x^*	[nm]	553	391	332	235	196	126	40.4	26.7
σ_y^*	[nm]	5	2	5	4	4.5	2.7	0.6	0.45
Υ		0.04	0.085	0.10	0.29	0.18	0.56	8.7	26.4
δ	[%]	2.6	4.4	3.8	9.1	3.6	9.2	32	42
n_γ		1.6	1.5	1.5	1.16	0.8	1.1	2.5	4.4
N_\perp		44	63	9.8	18.4	2.9	8.0	135	314
N_H		0.23	0.6	0.07	0.33	0.022	0.15	7.8	24
N_{MJ}	$[10^{-2}]$	0.61	3.1	0.20	2.3	0.08	1.27	13*	75*

E_{cm} : centre-of-mass energy, \mathcal{L} : actual luminosity, f_{RF} : acceleration frequency,
 G_{load} : loaded gradient, η : overall efficiency, f_r : repetition frequency,
 N_b : no of bunches per train, Δ_b : distance between bunches, N : no of particles per bunch,
 σ : bunch dimensions at IP, $\gamma\epsilon$: normalised emittances, Υ : average beamstrahlung parameter,
 δ : average energy loss, n_γ : no of photons per beam particle,
 N_\perp : no of particles from incoherent pair production with $p_\perp > 20$ MeV, $\theta > 0.15$,
 N_{Had} : hadronic events, N_{MJ} : minijet pairs $p_\perp > 3.2$ GeV/c (*numbers are for $p_\perp > 10$ GeV/c).

on luminosity and centre-of-mass energy of the different designs are discussed together with the rationales that drive the choices.

1.1 Basic Considerations

In linear colliders two different lower limits exist for horizontal and vertical spot sizes, for a beam with fixed charge and length. The horizontal limit stems from the so-called beamstrahlung, an intense radiation that is emitted by the particles of each colliding bunch in the strong field of the other one, as will be discussed later. The limit on the vertical beam size is due to the vertical emittance of the beam. If either bunch length or charge are varied, the related changes of the other parameters keep the geometric luminosity constant.

A number of parameters for the different designs is shown in Table 1. In all machines a number of bunches N_b , forming a train with a bunch separation Δ_b , is accelerated in a short RF-pulse in order to achieve high efficiency. The time between pulses exceeds the pulse duration $\Delta_b N_b$ by orders of magnitude. For small

beamstrahlung parameters Υ , as exist in all designs with $E_{cm} \leq 1$ TeV, one finds the luminosity to be roughly proportional to

$$\mathcal{L} \propto \frac{\sqrt{\delta}}{E_{cm}} \frac{\eta}{\sqrt{\epsilon_y}} P.$$

Here, δ is the average relative energy loss due to beamstrahlung, η the efficiency of turning wall plug power into beam power, ϵ_y the normalised vertical emittance and P the available wall plug power. Here, $\sqrt{\delta}/E_{cm}$ is fixed by physics, requesting a certain energy and quality of the luminosity spectrum. The available power is determined by boundary conditions from the outside (available budget). The term $\eta/\sqrt{\epsilon_y}$ is determined by the accelerator technology. The main linac, where the beam is accelerated, consumes most of the power, so it strongly affects η . The small beam emittance is achieved in the damping rings but the main source of emittance growth is the main linac.

1.2 Normal Conducting Designs

The different normal conducting studies are very similar in their overall design. The main parameter to be chosen is the acceleration frequency f_{RF} , in the optimisation process the other parameters tend to follow simple scaling laws [12]. Two very important parameters that follow from the frequency are the acceleration gradient and the alignment tolerances. For higher frequencies, it is possible to achieve higher gradients, which leads to a higher centre-of-mass energy for the same collider length. It is assumed that to reach high centre-of-mass energies at reasonable cost, high frequencies are therefore essential. On the other hand, high frequency leads to strong wakefields in the main linac. These wakefields will make it more difficult to preserve the emittance. While the wakefields rise drastically, all the other beam parameters (such as bunch length and charge) change in favour of the emittance preservation. The remaining effect can be prevented by aligning the linac more precisely. How much easier it is to align smaller components (partly using so-called beam based alignment) is subject to debate. Simulations assuming achieved alignment precisions predict sufficiently small emittance growth [3] [14].

Initially a wide range of frequencies has been investigated, reaching from 3 to 30 GHz. Now, the remaining major projects try to reach the highest frequency for their technology. In the case of NLC and JLC-X the aim is to use a conventional approach, where the acceleration power is provided by klystrons. Since the klystron technology becomes more difficult at higher frequencies, 11.4 GHz was chosen. Already at this frequency a very extensive klystron development programme is necessary, which is one of the major challenges of the two studies. Prototypes reached the required performance, but mass production studies are not completed. The gradient aimed for in the NLC is $G = 55$ MV/m allowing a 30 km long machine to reach $E_{cm} = 1$ TeV. In the planning, a first stage with $E_{cm} = 0.5$ TeV is foreseen. After the upgrade to $E_{cm} = 1$ TeV, a further upgrade to 1.5 TeV might be possible.

CLIC was from the very beginning aiming to very high energies, so that it can provide a wide physics reach after LHC. The frequency chosen is 30 GHz, at higher frequencies the production of the acceleration structures becomes significantly more difficult [13]. The acceleration power is provided by a drive beam which runs in

parallel to the main beam. This high-current low-energy beam is produced at low frequency and decelerated in power extraction and transfer structures. Each of these structures directly feeds two main linac structures where the low-current high-energy main beam is accelerated. Details of the power generation scheme can be found in a report [15]. With a gradient of $G = 150 \text{ MV/m}$ a centre-of-mass energy of $E_{cm} = 3 \text{ TeV}$ can be reached with a 35 km long machine.

1.3 Superconducting Design

In the case of TESLA the gradient is not limited by the frequency but rather by the properties of the superconductor. If the magnetic field in the superconductor, induced by the accelerating field, exceeds a certain limit, superconductivity breaks down. Increasing the frequency does not allow higher gradients to be reached. TESLA operates therefore at the lower frequency of 1.3 GHz. The wakefields are thus very small, while the gradient of 21.7 MV/m is higher than in a normal conducting design of the same frequency. This leads to a very small emittance growth in the main linac which allows a very high luminosity to be reached, see Table 1. In addition the superconducting acceleration is more efficient than in the normal conducting designs.

The machine is designed for $E_{cm} = 0.5 \text{ TeV}$, with an upgrade option to $E_{cm} = 0.8 \text{ TeV}$. This requires the gradient to be increased from about 21.7 MV/m to 34 MV/m. The first gradient has been achieved in a number of structures [16]. Significant cost reduction for the structures compared to previous projects is essential.

Because of the very high Q -value of the cavities, the pulse length is 0.8 ms in TESLA, leading to a bunch-to-bunch distance of about 300 ns, compared to only 0.67–2.8 ns in the other designs. This offers advantages for the machine and the experiment. In the machine it is possible to use feedbacks during the pulse to correct for most machine aberrations. In the detector individual bunch crossings can be separated, simplifying the physics analysis.

2 Pinch Effect and Beamstrahlung

A detailed introduction to the beam-beam effects and resulting background can be found elsewhere [17] [18].

2.1 Pinch Effect

The electro-magnetic fields in the bunches are very strong due to their small size. While within a bunch the electric and the magnetic forces almost cancel, they add for the oncoming bunch. If the two beams have different signs of charge the forces are attracting, each bunch will focus the oncoming one. The forces are strong enough to change the transverse sizes of the bunches significantly during the interaction. This enhances the luminosity \mathcal{L} compared to the geometric one \mathcal{L}_0 and makes the interaction quite complicated. It is therefore necessary to simulate the pinch effect. The two main codes CAIN¹ [19] and GUINEA-PIG [21] are in good agreement with measurements of H_D at the SLC [22]. For the present designs, the luminosity enhancement factor $H_D = \mathcal{L}/\mathcal{L}_0$ is about $H_D \approx 1.5 - 2$.

¹CAIN is the successor of a code named ABEL [20] which it is meant to replace.

2.2 Beamstrahlung

Since the beam particles travel on curved trajectories they emit radiation, the so-called beamstrahlung. This is essentially the same as synchrotron radiation and can be described with the beamstrahlung parameter $\Upsilon = 2/3 \cdot \langle E_c \rangle / E_0$, the ratio of the average critical energy $\langle E_c \rangle$ to the beam energy E_0 . For the designs with $E_{cm} \leq 1$ TeV, this is smaller than one, at $E_{cm} = 3$ TeV it is much larger, see Table 1. The number of photons emitted n_γ is usually of the order of one, so the stochastic nature of the process has to be taken into account. Beamstrahlung changes the luminosity spectrum significantly, since the particles lose from a few to many percent of their energy (2.8 % in TESLA at $E_{cm} = 0.5$ TeV to 42 % in CLIC at $E_{cm} = 5$ TeV). For the designs at $E_{cm} = 0.5$ TeV, the effect of the beamstrahlung on the spectrum is comparable to the one of initial state radiation. At higher energies it is less strongly peaked.

The beamstrahlung photons represent also a significant power (300 kW in case of TESLA at $E_{cm} = 0.5$ TeV and 5 MW in CLIC at $E_{cm} = 5$ TeV). Since the photons are emitted into a small angle into the forward direction, this is not a problem inside the detector. In the extraction beam line, however, special care has to be taken that they do not destroy components or induce high backgrounds.

The photons from beamstrahlung can also collide with photons or particles of the other beam, producing background, as will be discussed below.

2.3 Coherent Pair Creation

In a strong electro-magnetic field, a photon can turn into an electron-positron pair. The probability for a photon of energy $\hbar\omega$ to turn into a pair depends on $\kappa = \hbar\omega/E_0\Upsilon$. It is exponentially suppressed for $\kappa \ll 1$, while for κ approaching or exceeding one it is large. For CLIC at $E_{cm} = 0.5$ TeV one finds 3.4 pairs per bunch crossing from this process. At $E_{cm} = 1$ TeV the number reaches $2 \cdot 10^5$ and therefore becomes important as a background source. At $E_{cm} = 3$ TeV and $E_{cm} = 5$ TeV, $8 \cdot 10^8$ and $2.9 \cdot 10^9$ pairs are found. These numbers are not negligible compared to the bunch charge of $4 \cdot 10^9$ particles and therefore start to affect the beam-beam interaction itself. The spectrum of produced particles is shown in Fig. 1 for CLIC at $E_{cm} = 3$ TeV.

If an electron produced via pair creation flies in the direction of the electron beam, it is focused by the positron beam. If it goes the other way, it is deflected outwards by the electron beam, while the electric and magnetic forces of the positron beam cancel. Due to this deflection the particle can reach much larger transverse momenta than the beam particles of the same energy, which are always focused. Figure 1 shows the total energy of the particles from coherent pair creation as a function of the minimal particle angle after the beam crossing. In order not to lose too much energy in the detector region, which could lead to large number of secondaries, an exit cone of about 10 mradian has to be provided.

2.4 Luminosity Spectrum

Figure 2 shows the luminosity spectrum in CLIC at two different energies. Due to the large δ , it is significantly more degraded at the higher energy. By varying the horizontal beam size in the collision point, one can control the beamstrahlung. In

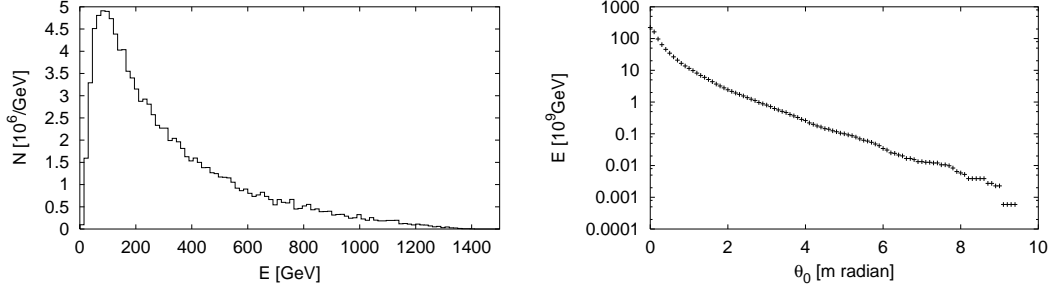


Figure 1: The energy spectrum for the particles due to coherent pair creation in CLIC at $E_{cm} = 3$ TeV; and the integral energy of the particles from coherent pair creation as a function of their minimal angle.

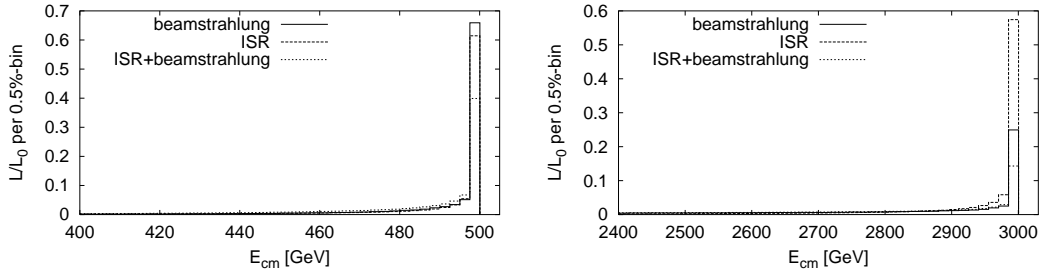


Figure 2: The luminosity spectrum in CLIC for $E_{cm} = 0.5$ TeV (left) and $E_{cm} = 3$ TeV.

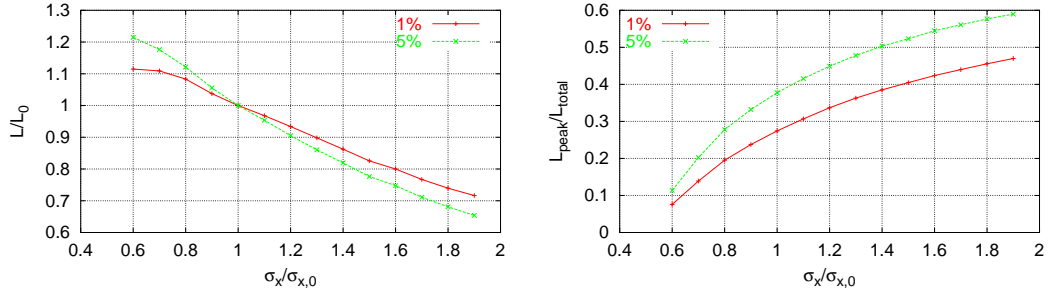


Figure 3: The absolute and relative luminosity in the peak of the spectrum in CLIC at $E_{cm} = 3$ TeV.

Fig. 3 this is exemplified. In the first part the absolute luminosity with $E_{cm} > 0.99E_{cm,0}$ and $E_{cm} > 0.95E_{cm,0}$ is shown as a function of the horizontal spot size. Increasing the later by a factor 1.9 leads to a loss in luminosity at the peak of about 30 %. However, the peak then contains almost 50 % of the total luminosity rather than 27 % with the nominal parameters. The optimum choice depends on the requirements of the experiments and may vary from study to study.

The luminosity spectrum can be measured using Bhabha scattering. While it is very difficult to measure the energies of the scattered particles, the difference in the angle of the two scattered particles can be used [23]. From the transverse momentum conservation one can then obtain the ratio of the energies of the two colliding particles

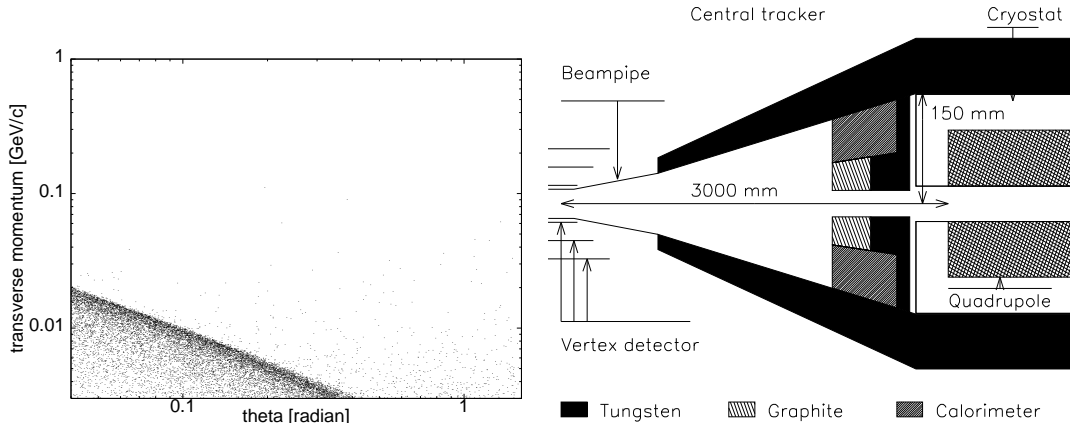


Figure 4: The particles from incoherent pair creation after the crossing of the bunches in TESLA. On the right side, the layout of the mask in TESLA. The vertical dimension is enhanced.

$E_1/E_2 = \sin \theta_1 / \sin \theta_2$. In addition a spectrometer can be used to measure the mean energy and the energy distribution of the beams before and after collision.

3 Detector and Background

3.1 Incoherent Pair Production

Three main processes lead to the incoherent production of e^+e^- pairs; the Landau-Lifshitz ($ee \rightarrow ee + (e^+e^-)$), the Bethe-Heitler ($e\gamma \rightarrow e + (e^+e^-)$), and the Breit-Wheeler process ($\gamma\gamma \rightarrow (e^+e^-)$). Here, the real photons are due to beamstrahlung. All these processes can be easily calculated using the equivalent photon approximation to replace initial electrons or positrons. The number of particles produced per bunch crossing is given in Table 1. Again it is necessary to track the produced particles through the fields of the two beams. Each dot in Fig. 4 represents one particle after the bunches crossed. For the bulk of the particles a clear correlation between the maximum transverse momentum and angle reached is visible. The few particles above this edge were produced with large angles and transverse momentum. Those below the edge obtained most of their transverse momentum from the deflection by the beams.

It has to be avoided that the bulk of these particles hit the vertex detector. If the coverage of this detector is $|\cos \theta| < 0.98$, all particles with an angle of less than $\theta \approx 200$ mrad cannot reach it. This removes all particles left of a vertical line in Fig. 4. The longitudinal field in the detector, on the other hand, causes a particle to travel on a helix. If the radius of the detector is at least twice as large as the radius of this helix, it can not be hit. This removes all particles below a horizontal line in the figure. The combined effect is even more efficient. For CLIC at $E_{cm} = 3$ TeV, the density of particles that hit the vertex detector as a function of the detector radius is shown in Fig. 5 for different field strengths. One to a few hits per mm^2 are expected to be acceptable [25], so at $B_z = 4$ T a radius of 30 mm would be sufficient. In TESLA

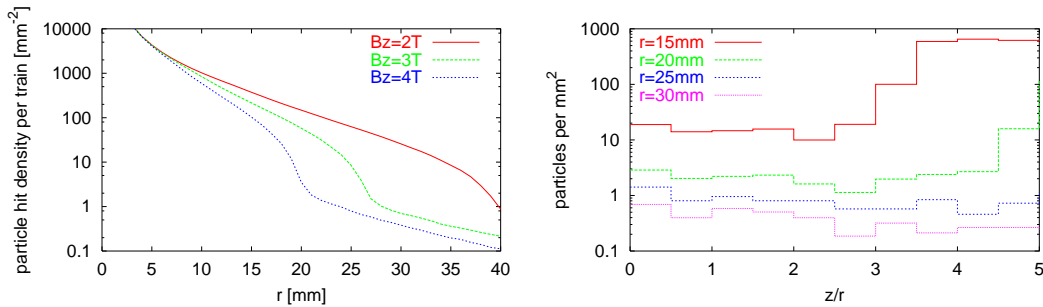


Figure 5: The particle density in the vertex detector of CLIC as a function of the detector radius and the longitudinal distribution for $B_z = 4$ T.

a radius of the innermost layer of 12 mm seems to be feasible with a fast readout.

Most of the particles from pair creation will hit the final quadrupoles, which are placed inside the detector. To avoid backscattered secondary photons in the detector, the quadrupoles have to be shielded by a tungsten mask, see Fig. 4. In the case of TESLA, the outer angle of this mask is $\theta_0 = 83$ mradian. Also low-energy charged particles can be backscattered. They are led by the field lines straight back into the interaction point region, and have a high probability of hitting the vertex detector [18]. This effect can enhance the number of background hits by an order of magnitude. To prevent this, the inner part of the mask is made out of tungsten covered by a low- Z material. If the radius of the inner mask is smaller than that of the vertex detector, almost complete suppression can be achieved.

3.2 Other Background Sources

Photon-photon collisions at the interaction point also lead to the production of hadrons. In Table 1 the number of hadronic events per bunch crossing with a minimum centre-of-mass energy of 5 GeV is shown. The cross section used is a pessimistic case from a parametrisation by G. A. Schuler and T. Sjöstrand [24] [21]. Precise numerical evaluation of the impact of this background on event reconstruction remains to be done for most measurements.

The neutron flux in the detectors is orders of magnitude smaller than the one in ATLAS or CMS. In the vertex detector of SLD charged coupled devices are used, reaching extremely good performance. These are very sensitive to neutrons, with a current limit of $3 \cdot 10^9$ neutrons per mm^2 [25]. The two main neutron sources are electro-magnetic showers, either induced by the pair particles hitting the final quadrupoles inside the detector, or by beam particles and beamstrahlung photons lost in the extraction line, outside of the detector. The latter can be shielded, with some difficulty for the vertex detector [18]. The flux from the first source seems to be below the limit [26] [18].

4 Conclusion

The different studies of future linear colliders have reached a high level of sophistication. In the framework of the different studies, test facilities have been build.

For TESLA and the NLC, design reports are being prepared that should be available in about two years from now. These reports will contain cost estimates. In the case of TESLA, a possible site close to Hamburg has been investigated and the legal procedures have started to obtain the necessary permit from local authorities (Planfeststellungsverfahren). For CLIC a new test facility is in the design stage, which will be presented in 1999 to the CERN management. This facility provides a test of the proposed power generation scheme, including all main components.

The study of the detectors is reaching a high technical level for $E_{cm} \leq 1$ TeV. Different generators for background exist and beamstrahlung has been implemented into some standard event generators, e.g. in PYTHIA [27] via CIRCE [28]. Costed detector proposals should be ready together with the machine proposals. For energies of $E_{cm} \geq 3$ TeV, a similar study is needed and should start soon, since feedback from physics and detector requirements on the collider parameters is essential.

References

A number of URLs is given, since they contain up to date information and allow access to programs.

References

- [1] E. Accomando et al. *Phys. Rep.* 299 (1998) 1–78.
- [2] R. Brinkmann et al. *DESY-1997-048* and *ECFA 1997-182*.
- [3] The NLC Design Group. *SLAC-Report 474*.
- [4] The report of the JLC Design Study Group can be found on <ftp://lcdev.kek.jp/pub/DesignStudy/>.
- [5] J.-P. Delahaye *PAC 1999* and *CERN/PS/99-05(LP)*.
- [6] <http://www.slac.stanford.edu/xorg/ilc-trc/ilc-trchome.html>
- [7] *DESY-123 A-E*
- [8] <http://www.desy.de/conferences/ecfa-desy-lc98.html>
- [9] <http://lcwws.physics.yale.edu/lc/america.html>
- [10] <http://acfahep.kek.jp/>
- [11] <http://lcwws.physics.yale.edu/lc/>
- [12] J.-P. Delahaye et al. *CERN/PS/97-51*.
- [13] I. Wilson. Private communication.
- [14] D. Schulte. *EPAC 1998 and CERN/PS/98-018*.
- [15] H. H. Braun et al. *CLIC-Note 364*.

- [16] M Pekeler. *EPAC 1998*
- [17] P. Chen, K. Yokoya. *KEK Preprint 91-2*.
- [18] D. Schulte. *Ph.D. thesis, University of Hamburg* and *TESLA-97-08*.
- [19] Program is developed by K. Yokoya and others, see
<http://www-acc-theory.kek.jp/members/cain/>.
- [20] K. Yokoya. *KEK-Report 85-9*.
- [21] D. Schulte. *ICAP 1998* and *CERN/PS/99-014 (LP)*.
- [22] N. Phinney. *PAC 1999*.
- [23] M. N. Frary and D. Miller. *DESY 92-123-A (1992)*.
- [24] G. A. Schuler and T. Sjöstrand. *CERN-TH/96-119*.
- [25] C. Damerell. Private communication.
- [26] N. Tesch. Private communication.
- [27] <http://www.thep.lu.se/~torbjorn/Pythia.html>
- [28] <http://heplix.ikp.physik.tu-darmstadt.de/nlc/beam.html>